River Flow 2010 - Dittrich, Koll, Aberle & Geisenhainer (eds) - © 2010 Bundesanstalt für Wasserbau ISBN 978-3-939230-00-7

A synthetic method for assessing small dams flood wave

S. Grimaldi & D. Poggi
Dipartimento di Idraulica Trasporti ed Infrastrutture Civili, Politecnico di Torino, Torino, Italy.

ABSTRACT: Flood inundation due to dam failure may cause loss of lives as well as widespread damages. According to recent changes in dam safety policy in Italy, regional authorities are required to build their own laws regulating risk analysis of small dams. It is well known that a proper and rigorous analysis should involve dam break flood wave modeling. Nevertheless, analytical solutions for dam break waves badly fit real cases and numerical modeling is very expensive in terms of both data entry and time. The large number of small dams built in Europe requires a simple but scientifically based methodology to assess flood wave routing. Referring to Piedmontese (Italy) dams many simple but representative models of reservoirs and downstream valleys were built; the complete modeling of several dam break waves was achieved using the numerical code BreZo 4.0. By means of this numerical lab a) finite basin length, b) geometric and hydraulic reservoirs features, and c) valley characteristics influence on dam-break waves were pointed out. This paper proposes a simple, effective, synthetic, physically based protocol to quickly assess flood wave arrival time and peak discharge values at each point downstream of the dam.

Keywords: Synthetic methodology, Numerical analysis, Dam failures, Flood routing, Hydraulic and geometric properties

1 INTRODUCTION

A dam failure may release large quantities of water that create major flood waves in the tail water and cause loss of lives and serious damages. Singh (1996) has noted 1000 dam failures since the 12th century; about 200 have occurred in the 20th century causing a loss of more than 8000 lives and damage worth millions of dollars.

Risk analysis assessment of existing dams is thus a central feature for both land use management and emergency planning. Risk analysis concepts for evaluation of existing dams safety have been widely studied and applied in the last three decades (Federal Coordinating Council for Science, 1979; Gruetter and Schnitter, 1982; Atkinson and Vick, 1985; US Bureau of Reclamation, 1989; Nielsen, 1993; Salmon and Hartford, 1995; Hartford and Nielsen, 1995; Rodriguez, 2002). According to the results of different dam break scenarios risk zones are identified with respect to the elapsed time between the dam failure and the arrival of dam break induced flood wave as well as wave intensity at a certain cross section (Rodriguez, 2002). Referring to RESCDAM Final Report of December 2000, wave intensity at each downstream cross section depends on peak discharge value. Dam break waves modeling is extremely important in providing the information needed for risk assessment and management of river valleys.

Starting from the milestone contribution by Ritter (1892), many analytical solutions were proposed. Briefly, we can list analytical solutions due to Dressler (1952), Whitham (1955), Stoker (1957), Su & Barnes (1970), Hunt (1982-84), Hunt & Gozali (1993), Chanson (2009). All these theories avoid the disturbance effects due to a finite basin length. Hogg (2006) first focused on the reservoir emptying process and the disturbance effects due to the presence of a wall at the rear of the lock; nevertheless Hogg's analytical solution applies only for smooth, horizontal channel.

Although many studies aimed at improving the numerical aspects of dam break waves, physical modeling is relatively limited despite basic experiments due to Schocklitsch (1917), Levin (1952), Dressler (1954), US Corps of Engineers (1960),

Faurè and Nahas (1961), Cavaillè (1965), Estrade (1967), Chervet & Dallves (1970), Drobir (1971), Barr & Das (1980), Martin (1981), Miller & Chaudrhry (1989), Lauber & Hager (1997), Chanson et al. (2000), Briechle & Koteger (2002), Leal et al. (2002).

In recently years the emphasis has shifted toward numerical solutions such as those given by Sakkas and Strelkoff (1973,1976), Strelkoff, Schamber & Katopodes (1977), Chen (1980), Chen & Armbruster (1980), Fread (1982), Zoppou & Roberts (2000); ICOLD Bulletin 111 (1998) listed 27 numerical models. Numerical modeling is based on approximate solution techniques and it is validated by experimental or real data sets. Nevertheless a strict numerical modeling is very expensive in terms of both data entry and time. The large number of small dams built in Europe requires a synthetic but scientifically based methodology to assess main dam break flood wave features, i.e. wave arrival time and peak discharge values.

A proper analysis of Piedmontese dams (Italy) allowed to build many simple but representative models of reservoirs and valleys features. The numerical code *BreZo 4.0* (Begnudelli & Sanders, 2006) was used for the complete modeling of several dam break waves. Based on this numerical lab, the main features of dam break flood wave were investigated and pointed out. In order to consider the worst scenario and achieve upper boundary solutions a total instantaneous collapse on a dry bed channel was assumed. Focusing on the disturbance effect due to the limited reservoir extension as well as morphology and hydraulic parameters, this paper presents a simple but scientifically based methodology to assess wave arrival time and peak discharge values.

2 BASIC EQUATIONS

A dam break wave is the flow resulting from a release of a mass of fluid in a channel witch generates a flood wave propagating in the tail water valley and a negative wave propagating up along the reservoir. The stream wise length scale of the motion is usually assumed to be much greater than the depth of the intruding current, so that the vertical fluid accelerations are negligible and the pressure is hydrostatic to leading order. With the further assumptions that drag forces may be neglected and that the current does not mix with the ambient, the motion may be modeled by the shallow water equations (Whitham, 1974). Thus aligning the x-axis with the direction of propagation and denoting the downstream cross section area with Ω , the flow depth and discharge by h and q, respectively, we find that

$$\begin{cases} \dfrac{\partial q}{\partial x} + \dfrac{\partial \Omega}{\partial t} = 0 & \text{(1a)} \\ \dfrac{1}{\Omega}\dfrac{\partial q}{\partial t} + \dfrac{1}{\Omega}\dfrac{\partial}{\partial x}\left(\dfrac{q^2}{\Omega}\right) + g\dfrac{\partial h}{\partial x} - gi_f - gj = 0 & \text{(1b)} \end{cases}$$

Local acceleration term	Convective acceleration term	Pressure force term	Gravity force term	Friction force term

where i_f is the bed slope and j is the friction slope. The shallow water equations (1) cannot be solved analytically because of nonlinear terms, e.g. the friction slope j .

Dam break wave modeling is often based upon numerical predictions. Referring to experimental and real data sets results, we used the numerical code *BreZo 4.0* due to Begnudelli & Sanders (2006). *BreZo 4.0* solves the shallow-water equations using a Godunov-type finite volume algorithm that runs on an unstructured grid of triangular cells and was optimized for wet and dry conditions. By means of this software forecasts of the flood wave under different hypothesis can be set up, simulated and analyzed.

3 MODELS DESCRIPTION

A physically based study on dam break flood routing parameters involves the definition of many simple but representative models of both dams and downstream valleys features. A recently developed survey on Piedmontese dams provided the database required. Although Piedmontese dams are 612, only a few geometric parameters are known: reservoir volume (511 values) and area (148 values); dam height (513 values) and width (323 values). Furthermore only 148 dams own the whole set of parameters while 296 dams are described by reservoir volume, dam height and width values. Hence very little information is often available; a suitable methodology must require few parameters. A proper analysis of Piedmontese dams and valleys features allowed to build many simple but representative models.

3.1 *Reservoir geometry*

Both numerical and experimental dambreak studies usually use wedge shaped reservoirs whose bed slope equals downstream valley slope i_f, nevertheless our analysis highlighted that a parallelepiped can properly fit several reservoirs shape. Figure 1 shows the Piedmontese reservoir shape probability density frequency curve. A shape

coefficient k (2) was defined as the ratio between measured a_{ms} and modeled a_{md} values of basin area a.

$$k = a_{ms} / a_{md} \quad (2)$$

Modeled area values a_{md} are computed as the ratio between reservoir volume and height values (3).

$$a_{ms} = v / h_o \quad (3)$$

Referring to many simple solids, the shape coefficient k equals 0.75 for an ellipsoid quarter, 1 for a parallelepiped, 1.5 for a rectangular based pyramid, 2 for a wedge, 3 for a triangular based pyramid. Based on the database supplied, the probability density function of k values pointed out that the largest fraction of Piedmontese dams has a parallelepiped shape.

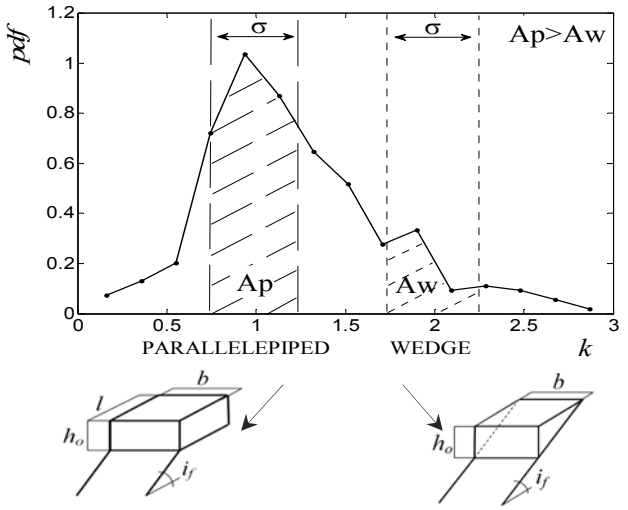

Figure 1. Piedmontese reservoirs shape probability density frequency curve

Despite the former hypothesis of a wedge shaped reservoir, one more parameter, i.e. the reservoir length l, is required in addition to dam height h_o and width b values in order to completely define the geometry of a parallelepiped-shaped reservoir.

On the basis of a statistic analysis of Piedmontese reservoirs typical upstream length l, dam height h_o and width b were used in order to build our numerical lab.

3.2 *Downstream geometry*

To minimize the natural flood wave attenuation effect a downstream prismatic channel as wide as the dam (b), with uniform slope i_f and roughness n was used. Valley parameters values were defined referring to Piedmontese downstream land features. We pointed out downstream valley slope values using ArcGis instruments. A proper statistic analysis defined the range of values to be used in our models. Previous experimental studies due to Fabrizio & Bianco (2002) pointed out a few equations to assess valley roughness as a function of bed slope values.

3.3 *Dambreak mechanism*

A total instantaneous collapse represents the worst scenario. Since the base flow in such a case can often be neglected, the dam-break wave propagates over a dry bed. This hypothesis is not intended to be exhaustive but it allows the assessment of upper boundary values of flood wave arrival time and peak discharge. Furthermore the analysis herein developed provides a reference to further studies on partial, gradual dam break scenarios.

4 DAM BREAK FLOOD WAVE ROUTING

A sudden release of a mass of fluid in a channel generates a flood wave propagating in the tail water valley and a negative wave propagating up along the reservoir. When the dam is instantaneously removed there is a rarefaction wave centered at the dam section ($x=0$) and the motion is unaffected by the finite length l of the reservoir until the first backward-propagating wave has reached the rear of the lock. Thereafter the flow becomes affected by the finite basin length. As far as the first negative wave reaches the reservoir upstream cross section, it is reflected downstream. Whenever the disturbance due to the reservoir finite length catches up with the front wave, it affects the flood wave routing both in terms of arrival time and peak discharge values.

Using *BreZo 4.0* and the information of the Piedmontese dams a numerical lab was built to investigate dam break flood wave routing main parameters, i.e. negative, positive wave, and peak discharge celerity as well as peak discharge values.

4.1 *Wave time arrival*

4.1.1 *Negative wave celerity*

The simple reservoir morphology with a constant depth yields to a constant value of the negative front wave celerity c_{NF} depending exclusively on the dam height h_o (4)

$$c_{NF} = \sqrt{g \cdot h_o} \quad (4)$$

Our numerical analyses yielded to an identical result to that proposed by Ritter (1892).

4.1.2 *Front wave and peak discharge celerity*

Referring to a two-dimensional simulation of flooding from the 1928 failure of St.Francis dam in southern California, Begnudelli & Sanders (2007) demonstrated that their numerical code BreZo 4.0 over predicts the speed of the flood wave by a significant factor; nevertheless peak discharge arrival time prediction appears much more accurate.

Actually, CADAM Final Report of January 2000 pointed out that all the numerical models analyzed, i.e. the numerical codes listed in ICOLD Bulletin 111 (1998), fail to predict the front wave celerity, and there isn't a clear relationship between wave speed, results accuracy and method adopted.

A dam failure flood hydrograph generally has a sharp rising limb with a very short interval between the initial discharge rise and the peak outflow. As a consequence the arrival time of a properly defined characteristic discharge value may represent both front wave and peak outflow arrival time. Referring to Lauber and Hager's experimental studies on the positive wave celerity (1998), we defined the characteristic discharge value q_c as a fraction of the maximum outflow at the dam site q_{dam}, i.e. the outflow at the dam site ($x=0$) at the collapse time ($t=0$):

$$q_c = 0.05\, q_{dam} \tag{5}$$

In case of total failure Ritter's analytical solution (1892) allows q_{dam} evaluation as (6)

$$q_{dam} = \frac{8}{27} \cdot g^{\frac{1}{2}} \cdot b \cdot h_o^{\frac{3}{2}} \tag{6}$$

Our numerical lab proved eq. (6) effectiveness.

4.1.2.1 Infinite reservoir length

As explained earlier the perturbation due to the reservoir finite length may affect the arrival time value. The implementation of a theoretical unlimited reservoir upstream length avoids the negative wave reflection at the upstream reservoir wall.

Referring to Piedmontese dams and valleys features we demonstrated that a total, instantaneous collapse involves, almost in its earliest phases, a supercritical flow. According to hydro-dynamics theory derivative terms of momentum equation (1b) in shallow water equations, i.e. acceleration and pressure terms, are negligible and friction and mass forces lead the motion. The resulting wave is called kinematic; the conceptually simpler kinematic model states that the flow is steady for momentum conservation while unsteady effects are taken into account through the continuity equation. The resulting quasi-linear hyperbolic differential system has analytical solutions. Referring to a rectangular prismatic channel equation (7) allows the evaluation of the celerity c_q of a constant discharge q.

$$c_q = \frac{dx_q}{dt} = \alpha^{-1} \cdot \left(\frac{n \cdot b^{2/3}}{i_f^{1/2}} \right)^{-1} \cdot q^{2/5} \tag{7}$$

Our numerical lab demonstrated equation (7) effectiveness in predicting the celerity of the characteristic discharge q_c provided that

$$\alpha = \frac{3}{8} \tag{8}$$

Figure 2 compares numerical model and analytical equations (5-6) results.

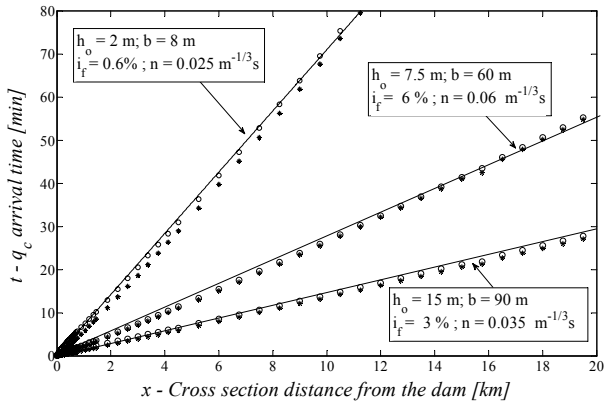

Figure 2. Numerical model (BreZo): positive front (*), peak discharge (o) arrival time; analytical model (eq.7,8): characteristic discharge q_c (—) arrival time

4.1.2.2 Finite reservoir length

A more realistic finite upstream length requires to focus on the disturbance due to negative waves upstream reflection and downstream routing. Figure 3 shows the limited basin effect on flood hydrograph at the dam site.

Although curve "a_{dam}" has a monotone decreasing trend, curve "b_{dam}" shows a flex point and a concavity change. Curve "b_{dam}" lays on curve "a_{dam}" as far as at time t_l , i.e. as far as the first reflected negative wave reaches the dam site. For time t greater than t_l curve "b_{dam}" shows a concavity change and a downward translation. The reservoir depth attenuation neglectivity allows to evaluate the characteristic time t_l as (9)

$$t_l = \frac{2 \cdot l}{\sqrt{g \cdot h_o}} \tag{9}$$

Since the reservoir is parallelepiped-shaped the first instant at which the flow is affected by the rear of the lock depends exclusively on dam height and basin length.

For time t greater than t_l the disturbance generated by the rear of the lock travels downstream: as far as it reaches the front wave it affects the flood wave routing. In Figure 3 curves "a_{max}" and "b_{max}" represent the peak discharge values evaluated at many downstream cross sections as a function of time. Provided that we replace the reservoir characteristic time t_l with a greater value t_D, curves "a_{max}" and "b_{max}" behave exactly like curves "a_{dam}" and "b_{dam}".

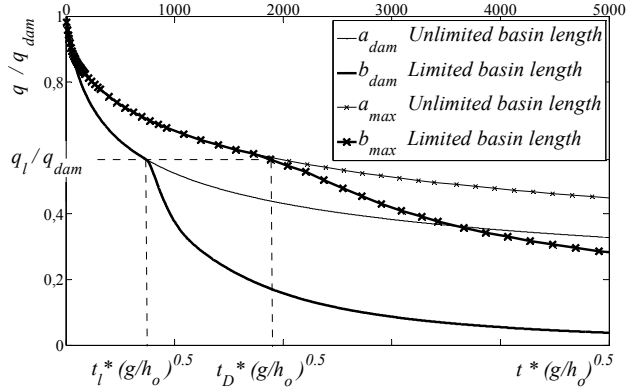

Figure 3. Limited basin effect on dam site hydrograph and peak discharge attenuation.

Figure 4 shows the disturbance routing; as explained later we refer to the disturbance discharge as q_l . Obviously, although such disturbance has effects on each hydrograph, maximum discharge value is affected by reservoir emptying process despite that the laps of time employed by the negative wave to arrive at the basin upstream cross section, reflect and reach the cross section itself is smaller than the peak flow arrival time.

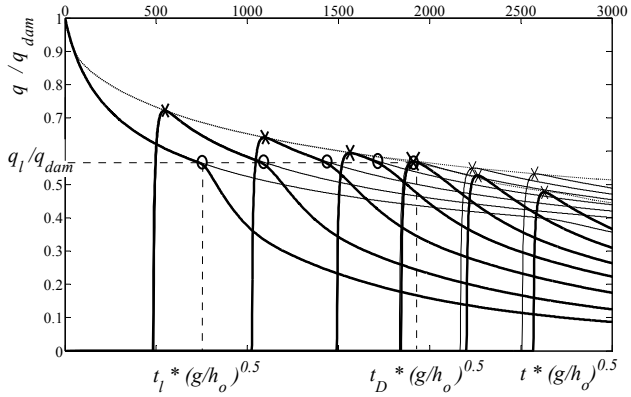

Figure 4. Disturbance effect routing.

Since diffusive terms, i.e. acceleration and pressure terms, of the momentum equation (1b) are negligible, mass and friction force terms lead the quasi-steady motion and the kinematic model properly describes the flood wave routing. Hunt (1982) showed how kinematic model can be used to obtain closed-form approximations; calculations and experiments suggesteed that these kinematic wave solutions become valid after the shock has traveled a number of reservoir lengths downstream.

Our numerical analyses pointed out that the disturbance discharge q_l is constant and equals dam site discharge value at time t_l.

Referring to the kinematic model, equation (7) allows the evaluation of the celerity of a constant discharge. Numerical efforts pointed out equation (7) effectiveness provided that (10)

$$\alpha = \frac{3}{5} \tag{10}$$

As stated so far, equations (7, 8) and (7, 10) respectively allow the evaluation of flood and disturbance wave celerities: Figure 6 shows that point D (x_D, t_D) named detachment point is the only common solution. The detachment point D marks both the first instant and the nearest location to the dam at which the peak discharge is affected by the presence of the rear wall of the lock.

Obviously the assessment the reservoir emptying disturbance celerity requires the evaluation of the disturbance discharge value q_l. The assessment of the discharge value q_l requires the reservoir emptying equations. In case the flow is supercritical the downstream flood routing doesn't have any influence upstream and the reservoir geometric and hydraulic features, i.e. dam height and width and basin length and roughness, lead the emptying hydrograph. On the contrary, in case the downstream flow is subcritical it influences upstream motion and the reservoir emptying depends both on reservoir and downstream valley features. We developed our numerical analyses referring to the former condition and the hypothesis of a flat downstream valley. A barely flat downstream valley provides the limit solution for the latter hypothesis; intermediate conditions of subcritical flow lay between the previous conditions.

According to our analyses, for small times Dressler theoretical solution (1952) fits numerical results both in case of subcritical and supercritical flows (equations 13, 16). Referring to larger times our numerical lab yielded to equations (14), (15) for a supercritical flow and to equations (17), (18) in case of a barely flat downstream valley. The Appendix lists the analytical equations pointed out; we normalized discharge values $q(x=0,t)$ and time values t according to Dressler theory (11,12)

$$Q(x=0,t) = \frac{q(x=0,t)}{q_{dam}} \tag{11}$$

$$T = t \cdot \sqrt{\frac{g}{h_o}} \tag{12}$$

Although in this paper we will exclusively use equations (13, 14, 15), Figure 5 shows numerical and analytical reservoir emptying hydrographs.

The flatter the valley, the greater the dam section discharge attenuation is.

The reservoir emptying perturbation makes the flood wave slow down and reduce its peak discharge values. Our numerical analyses highlighted that the dam height h_o as well as the basin length l are the flood routing leading parameters. Equation (19) allows the evaluation of the flood wave celerity for times t greater than t_D and cross sections x farter than x_D from the dam site.

$$\frac{x - x_D}{l} = 0.370 \cdot \sqrt{g \cdot h_0} \cdot \frac{t - t_D}{l} \tag{19}$$

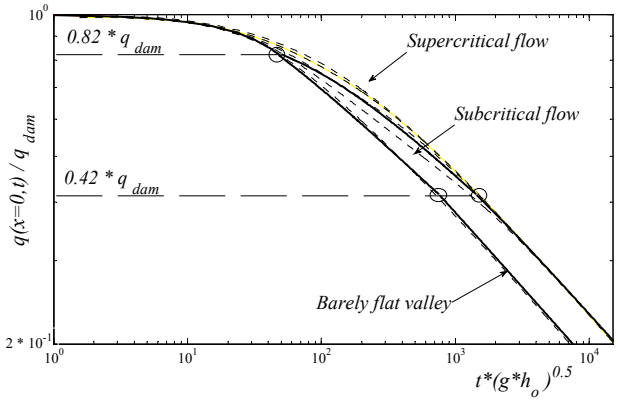

Figure 5. Reservoir emptying numerical (BreZo, ---) and analytical (—) hydrographs.

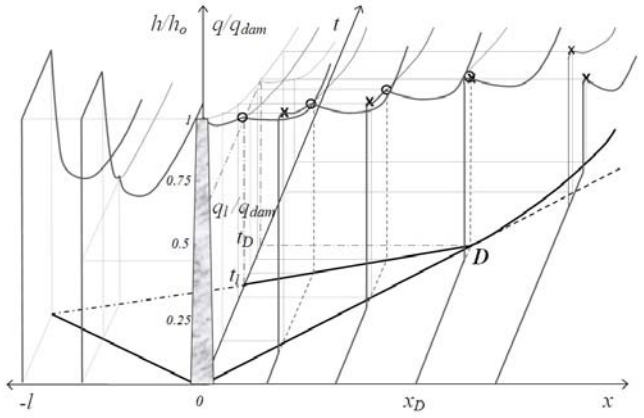

Figure 6. Negative wave, characteristic discharge, and disturbance wave routing.

4.2 *MAXIMUM DISCHARGE VALUES*

As mentioned earlier, flood wave intensity evaluation requires a procedure for estimating the maximum discharge at each cross section x far from the dam, q_{max} In the following, q_{max} will be normalized by q_{dam}. This approach allows us to focus on the factors affecting the wave attenuation effect. As mentioned earlier, according to both Ritter theoretical solution and our numerical analyzes q_{dam}, i.e. the discharge value at dam site $x=0$ at failure time $t=0$, equals (6):

$$q_{dam} = \frac{8}{27} \cdot g^{\frac{1}{2}} \cdot b \cdot h_o^{\frac{3}{2}} \tag{6}$$

4.2.1 *Total Collapse And Unlimited Reservoir Lenght:*

The implementation of a theoretical unlimited reservoir upstream length avoids the disturbance due to the wall at the rear of the lock and allows to focus on downstream valley parameters influence on peak discharge attenuation.

Numerical analyses pointed out that the ratio i_f / n^2 is the key parameter to describe the downstream land hydraulic features. Figure 7 shows the normalized discharge values of an unlimited reservoir as a function of downstream cross section distance from the dam. The smaller i_f / n^2 , the greater the influence of diffusive terms in momentum equation (1b), the larger the attenuation of the discharge hydrograph .

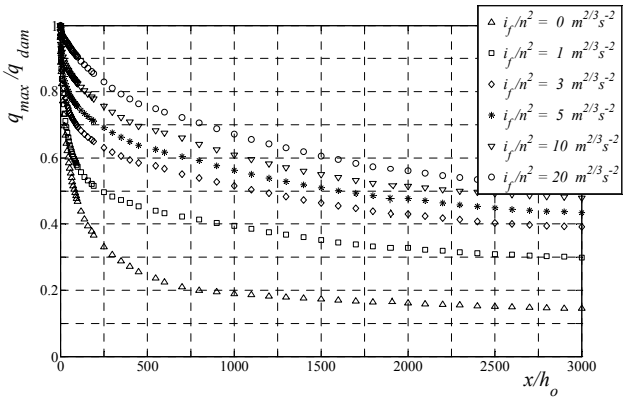

Figure 7. Downstream land hydraulic influence on peak discharge attenuation.

All the curves plotted have a monotone decreasing behaviour. In particular, this behaviour depends on downstream cross section distance x, dam height h_o, downstream land hydraulic features n, i_f (20); in general is:

$$\frac{q_{\max}}{q_{dam}} = f(x, h_o, n, i_f) \tag{20}$$

4.2.2 *Total Collapse And Limited Reservoir Length*

A more realistic finite upstream reservoir extension requires the introduction of the basin length l in equation (21).

$$\frac{q_{\max}}{q_{dam}} = f(x, h_o, n, i_f, l) \tag{21}$$

As explained earlier (Figure 3) curve "a_{max}" lays on curve "b_{max}" as far as the detachment point D, i.e. the cross section nearest to the dam affected by the disturbance due to the finite basin

length. The disturbance wave makes the flood wave slow down; the second most noticeable effect is a sensible increase in the flood wave peak attenuation.

In case the downstream cross section distance x is greater than detachment point distance from the dam x_D, our numerical analyses pointed out downstream cross section distance x , basin length l, downstream valley roughness n, and slope i_f as the leading parameters of the flood wave attenuation. Moreover, sensible changes in dam height h_o have no influence on peak discharge. Equation (22) reviews equation (21).

$$\frac{q_{\max}}{q_{dam}} = f(x, l, n, i_f) \tag{22}$$

Numerical efforts yielded to the analytical equation (23,24) listed in Table 2.

Table 2. Analytical equations to assess peak discharge values at each point downstream of the dam

Cross section distance	Equations
$x < x_D \Rightarrow$	
	$\frac{q_{\max}}{q_{dam}} = \alpha \cdot \left(\frac{x}{h_o}\right)^{\beta} + \gamma$ (23)
	$\alpha = -\frac{0.27}{0.30 \cdot \frac{i_f}{n^2} + 1}$ (23a)
	$\beta = \beta_1 \cdot \log\left(\frac{i_f}{n^2}\right) + \beta_2$ (23b)
	$\beta_1 = -0.00103 \cdot h_o + 0.08568$ (23c)
	$\beta_2 = 0.01088$ (23d)
	$\gamma = -\alpha + 1$ (23e)
$x > x_D \Rightarrow$	
	$\frac{q_{\max}}{q_{dam}} = \lambda \cdot \left(\frac{x}{l}\right)^{\delta}$ (24)
	$\lambda = 0.96010 \cdot \log\left(\frac{i_f}{n^2} + 1\right) + 0.12780$ (24a)
	$\delta = -1$ (24b)

As an example, Figure 8 shows numerical model and analytical equations results.

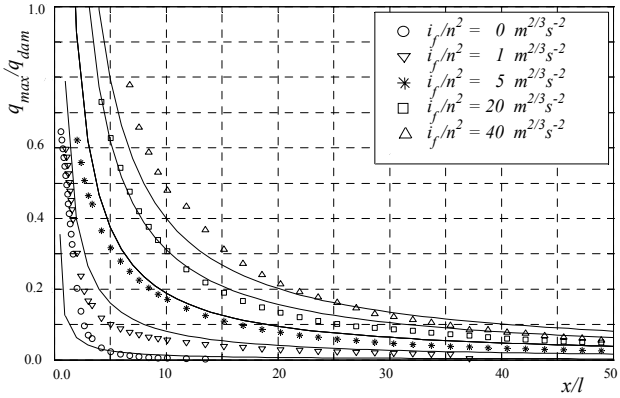

Figure 8. Numerical (BreZo, °) and analytical (eq. 24) behavior of the peak discharge attenuation for $x > x_D$.

5 DISCUSSION

Risk analysis assessment of existing dams is a central feature for both land use management and emergency planning. A proper risk analysis involves dam break wave modeling. Analytical solutions available badly fit real cases, while numerical modeling is very expensive in terms of both data entry and time; nevertheless the large number of small dams built in Europe requires a proper synthetic methodology. Referring to Piedmontese dams (Italy), many representative but simple models of dams and valleys features have been built. The complete modeling of dam break wave routing was achieved using the hydraulic software BreZo 4.0. By means of numerical analyses the key parameters leading flood wave routing were pointed out; in Figure 9. Evaluation of the degree of damage undergone by an urban area in case of total, instantaneous dam failure particular we focused on the disturbance effect due to the finite basin length. This paper proposes an original, simple, effective, synthetic, and physically based on statistic analys Figure 9. Evaluation of the degree of damage undergone by an urban area in case of total, instantaneous dam failures and hydraulic principles protocol to assess flood wave arrival time as well as peak discharge values at each point downstream of the dam. Previous studies pointed out the degree of damage caused to an element at risk as a function of flood wave intensity and arrival time. For instance, referring to RESCDAM Final Report of December 2000, Figure 9 shows that if a total, instantaneous dam failure occurs the urban area "Town" will undergo a major damage.

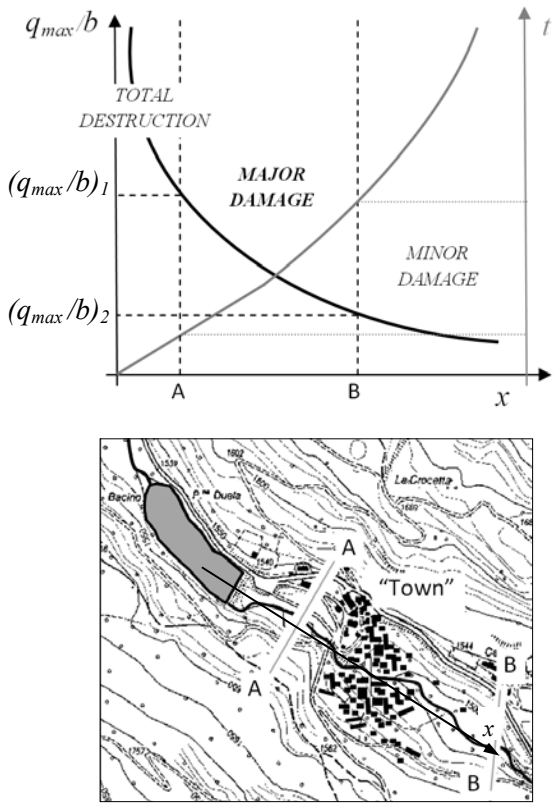

Figure 9. Evaluation of the degree of damage undergone by an urban area in case of total, instantaneous dam failure

APPENDIX:

Analytical equations for dam site hydrograph assessing.

SUPERCRITICAL FLOW

Discharge value	Equations
$1 \geq Q(x=0,t) \geq 0.82$	$Q(x=0,t) = 1 - 0.239 \cdot \frac{g}{\chi^2} \cdot T$ (13a); $\chi = \frac{1}{n} \cdot y_o^{1/6}$ (13b)
$0.82 \geq Q(x=0,t) \geq 0.42$	$Q(x=0,t) = \alpha_2 \cdot T^{\beta_2}$ (14); $\alpha_2 = \gamma_2 \cdot n^{\delta_2}$ (14a); $\gamma_2 = 0.05046 \cdot \log(h_o) + 0.5265$ (14b); $\delta_2 = -0.5300$ (14c); $\beta_2 = -0.2667$ (14d)
$Q(x=0,t) \leq 0.42$	$Q(x=0,t) = \alpha_3 \cdot T^{\beta_3}$ (15); $\alpha_3 = \gamma_3 \cdot n^{\delta_3}$ (15a); $\gamma_3 = 0.06193 \cdot \log(h_o) + 0.5872$ (15b); $\delta_3 = -0.6300$ (15c); $\beta_3 = -0.3200$ (15d)

SUBCRITICAL FLOW

Discharge value	Equations
$1 \geq Q(x=0,t) \geq 0.82$	$Q(x=0,t) = 1 - 0.239 \cdot \frac{g}{\chi^2} \cdot T$ (16a); $\chi = \frac{1}{n} \cdot y_o^{1/6}$ (16b)
$0.82 \geq Q(x=0,t) \geq 0.42$	$Q(x=0,t) = \alpha_2 \cdot T^{\beta_2}$ (17); $\alpha_2 = \gamma_2 \cdot n^{\delta_2}$ (17a); $\gamma_2 = 0.042591 \cdot \log(h_o) + 0.4401$ (17b); $\delta_2 = -0.5300$ (17c); $\beta_2 = -0.2667$ (17d)
$Q(x=0,t) \leq 0.42$	$Q(x=0,t) = \alpha_3 \cdot T^{\beta_3}$ (18); $\alpha_3 = \gamma_3 \cdot n^{\delta_3}$ (18a); $\gamma_3 = 0.05154 \cdot \log(h_o) + 0.4570$ (18b); $\delta_3 = -0.6300$ (18c); $\beta_3 = -0.3200$ (18d)

REFERENCES

Atkinson, G. and Vick, S. 1985. Risk Analysis For Dam Design. Proceedings of the H. G. Acres Seminar.

Begnudelli, L., Sanders, B. 2006. Unstructured Grid Finite-Volume Algorithm for Shallow Water Flow and Scalar Transport with Wetting and Drying. Journal of Hydraulic Engineering, 132(4), 371-384; DOI:10.1061/(ASCE)0733-9429(2006)132:4(371)

Begnudelli, L., Bradford, S., Sanders, B. 2008. Adaptive Godunov-Based Model for Flood Simulation. Journal of Hydraulic Engineering, 134(6),714-724; DOI: 10.1061/(ASCE)0733-9429(2008)134:6(714)

Begnudelli, L., Sanders, B.F. 2007. Simulation of the St.Francis Dam-Break Flood. Journal of Engineering Mechanics, ASCE, 133(11), 1200-1212; DOI: 10.1061/(ASCE)0733-9399(2007)133:11(1200)

Chanson, H. 2009. Application of the Method of Characteristics to the Dam Break Wave Problem. Journal of Hydraulic Research, IAHR, 47(1), 41-49; DOI: 10.3826/jhr.2009.2865

Fabrizio R. & Bianco G. La ricostruzione dell'andamento granulometrico lungo un corso d'acqua nell'ambito degli studi di idraulica fluviale. XXVIII Convegno di Idraulica e Costruzioni Idrauliche, Potenza 16-19 sept. 2002.

Gruetter, F., Schnitter, N. J. 1982. Analytical Risk Assessment for Dams. International Commission on Large Dams, Proceedings 14, International Congress on Large Dams, Rio de Janeiro, Brazil; Q.52, R.39.

Hogg, A. 2006. Lock-release gravity currents and dam-break flows. Journal of Fluid Mechanics, 569, 61-87; DOI: 10.1017/s00221-1200-6002588

Hunt, B. 1984. Perturbation solution for dam-break floods. Journal of Hydraulic Engineering, 110(6), 675-684; DOI ISSN 0733-9429/84/0006-0675

Hunt, B. 1984. Dam-Break solution. Journal of Hydraulic Engineering, 110(8), 1058-1071; DOI ISSN 0733-9429/84/0008-1058

Lauber, G., Hager, W. 1997. Positive front of dambreak wave. 27 IAHR Congress San Francisco, A: 729-733

Lauber, G., Hager, W. 1998. Experiments to dambreak waves: horizontal channel. Journal of Hydraulic research, 36(3), 291-307

Lauber, G., Hager, W. 1998. Experiments to dambreak waves: sloping channel. Journal of Hydraulic research, 36(3), 761-773

CADAM (Concerted Action on Dam Break Modeling). 2000. Final Report SR571.

ICOLD Bulletin 111. 1998. "Dambreak flood analysis-Review and recommendations".

Dressler, R.F. 1952. Hydraulic Resistance Effect upon the Dam-Break Functions. Journal of Research of the National Bureau of Standards, 49(3), 217-225.

Whitham, G. B. 1955. The Effects of Hydraulic Resistance in the Dam-Break Problem. Royal Society of London, Proceedings, Series A, 227, 399–407.

Ritter, A. 1892. The propagation of water waves. V.D.I. Zeitscher (*Berlin*) **,** 36(2), 947–954.

Whitham, G. B. 1974. Linear and Nonlinear Waves. Wiley.

Hunt, B. 1984. Perturbation solution for dam-break floods. Journal of Hydraulic Engineering, 110(6), 675-684; DOI ISSN 0733-9429/84/0006-0675

Ponce, V.M., Simons, D.B. 1977. Shallow wave propagation in open channel flow. Journal of the Hydraulics Division, ASCE, 103(HY12), 1461-1476.